Structural Eng./Earthquake Eng., JSCE, Vol. 14, No. 1, 1s-10s, 1997 January
(J. Struct. Mech. Earthquake Eng., JSCE, No. 556/ I -38)

# HARMONIC WAVE RESPONSE ANALYSIS OF ELASTIC FLOATING PLATES BY MODAL SUPERPOSITION METHOD

Chong WU[1], Tomoaki UTSUNOMIYA[2] and Eiichi WATANABE[3]

[1]Student Member of JSCE, Master of Eng., Dept. of Civil Eng., Kyoto University
(Yoshida-Honmachi, Sakyo-ku, Kyoto, 606-01, Japan)
[2]Member of JSCE, Dr. of Eng., Dept. of Civil Eng., Kyoto University
(Yoshida-Honmachi, Sakyo-ku, Kyoto, 606-01, Japan)
[3]Member of JSCE, Ph.D, Dr. of Eng., Dept. of Civil Eng., Kyoto University
(Yoshida-Honmachi, Sakyo-ku, Kyoto, 606-01, Japan)

This paper presents the modal superposition method in the application of wave-induced response analysis of mat-like floating plates. This method separates the coupled hydroelastic problem into uncoupled usual hydrodynamic problem and structural dynamic problem by expanding the motion of the plate as a superposition of modal functions which include rigid-body motions and bending modes of the plate. Effects of important parameters such as wave period, direction of incident waves and plate rigidity on the response of the plate are discussed. Comparisons between the two-dimensional analytical solutions and the three-dimensional solutions are also made.

***Key Words:*** *hydroelasticity, floating structure, plate, wave force, wave response, boundary element method, modal analysis method*

## 1. INTRODUCTION

In recent years, floating airports have been attracted considerable attention because of the fact that it is difficult to find a place on land or shallow sea for such purposes in Japan. Usually, pontoon type floating airports have large dimensions in length and width with compared to height. For example, the concept design of floating airport for Kansai international airport has a length of 4000m, a width of 1250m and a height of 4.5m[1]. Therefore such floating structures must be very flexible and the elastic deformations due to waves become significant. The interaction between structural deformations and waves must be taken into account in the design of such floating structures.

For solving this problem, several studies have treated the structure as a beam with free ends in two-dimensional fluid field, and the numerical solutions are in good agreements with the experimental results.[2)-7)] However, it is impossible to consider the influence of the incident direction of incoming waves by these method. On the study of floating structures in three-dimensional fluid field, Wen[8)] has proposed a time domain integration method for the analysis of a rectangular plates in linear shallow water waves. Hamamoto, Takahashi and Tanaka[9)] have performed the response analysis of a circular floating plate subjected to wind-waves and seaquakes. Mamidipudi and Webster[10)] have presented a combined method of singular point distribution method and finite difference method for analyzing the motion of a mat-like floating plate in wave. Newmen[11)] has extended the formulations of the linear potential theory from the rigid-body motion analysis to the generalized modal motions of various deformable bodies. Wang and Ertekin *et al.*[12)] have presented a hydroelastic-response analysis of a box-like floating airport of shallow draft.

This paper presents the modal superposition method in the application of wave-induced

harmonic response analysis of mat-like floating plates. This method separates the coupled hydroelastic problem into uncoupled usual hydrodynamic problem and structural dynamic problem by expanding the motion of the plate as a superposition of modal functions which include rigid-body motions and bending modes of the plate. The diffraction problem and the radiation problems are solved by the boundary integral equation method, and the hydroelastic equation of motion is solved by the Galerkin's method. The method is based on the assumptions of the linear wave theory and small amplitude motion of the structure. Some numerical examples show that this method converges rapidly.

Effects of some important parameters such as wave period, direction of incident waves and plate rigidity on the response of the plate are observed by the proposed method. Comparisons between the two-dimensional analytical solutions[7] and the three-dimensional solutions by the proposed method are also made.

## 2. GOVERNING EQUATIONS

The fluid-structure system is shown in **Fig.1**. The two horizontal coordinate axes, $x$ and $y$, are set to be parallel to the two sides of the plate and $x$-$y$ plane is on the mean position of the free surface of the water. The $z$-axis is pointing upwards and passing the center of the plate. The fluid is assumed to be incompressible, inviscid and irrotational so that the velocity potential exists. The waves and the motions of the structure are of small amplitude and only the vertical motion is considered.

Under the assumptions stated above, the flow can be expressed by a velocity potential, $\Phi(x,y,z,t)$, as

$$\Phi(x,y,z,t)=\mathrm{Re}\left(\phi(x,y,z)e^{-i\sigma t}\right) \tag{1}$$

and the steady-state vertical motions of the structure, $W(x,y,t)$, should be harmonic and can be expressed as

$$W(x,y,t)=\mathrm{Re}\left(w(x,y)e^{-i\sigma t}\right) \tag{2}$$

where $i$ is imaginary unit, $t$ is time, $\sigma$ is the circular frequency, $\phi(x,y,z)$ is the complex potential, and $w(x,y)$ is the vertical complex displacement of the plate.

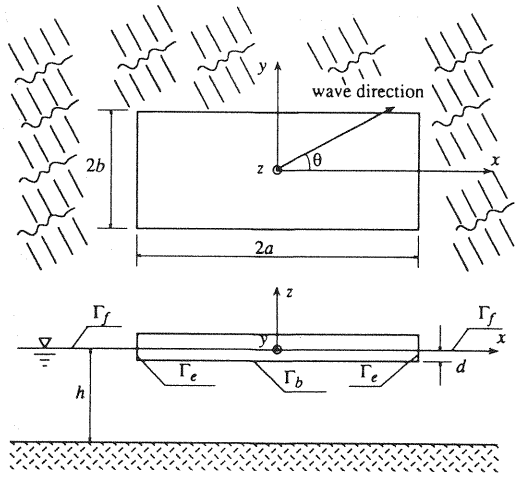


**Fig. 1** Fluid-structure system

The complex potential is governed by the Laplace's equation in the fluid domain

$$\nabla^2\phi=0 \tag{3}$$

and must satisfy the boundary conditions on the free surface, on the bottom and on the wetted surface of the body as

$$\frac{\partial\phi}{\partial z}=\frac{\sigma^2}{g}\phi \quad \text{on } \Gamma_f \tag{4}$$

$$\frac{\partial\phi}{\partial z}=0 \quad \text{on } z=-h \tag{5}$$

$$\frac{\partial\phi}{\partial n}=\begin{cases}-i\sigma w & \text{on } \Gamma_b\\ 0 & \text{on } \Gamma_e\end{cases} \tag{6}$$

where $g$ is the gravity acceleration, $h$ is the water depth, and

$$\frac{\partial}{\partial n}=n_x\frac{\partial}{\partial x}+n_y\frac{\partial}{\partial y}+n_z\frac{\partial}{\partial z} \tag{7}$$

in which $(n_x,n_y,n_z)$ is the unit normal vector pointing from the fluid domain into the body, $\Gamma_b$ and $\Gamma_e$ denote the wetted surface on bottom and side of the plate, respectively, $\Gamma_f$ is the free surface of the water.

The motion of the plate is governed by the thin-plate equation

$$\left(D\nabla^4 w\right)-\sigma^2 mw+kw=p \tag{8}$$

where $D$ is the plate rigidity, $m$ is the mass per unit area of the plate, $k$ is distributed restoring force factor,

$$\nabla^4 = \frac{\partial^4}{\partial x^4} + 2\frac{\partial^4}{\partial x^2 y^2} + \frac{\partial^4}{\partial y^4}, \tag{9}$$

$p$ is the wave pressure on the bottom of the plate given by the linearized Bernoulli's equation[13]

$$p = i\rho\sigma\phi \tag{10}$$

and $\rho$ is the density of the fluid.

## 3. EXPANSION OF MOTION

Exact solutions of the coupled hydroelastic equation (8) are generally difficult. On structural dynamics, the modal superposition method are widely used for analyzing the coupled vibrations of multi-degree of freedom system or continuous structures.. On hydrodynamics, this modal superposition scheme is successfully used by Newmen[11], Fathi[4] and Wu *et. al.*[7] to solve two-dimensional hydroelastic problems, and it is also employed by Wen[8] to analyze the response of a plate in linear shallow water waves.

The modal functions employed in this paper are as same as those which are used by Wen[8]. The displacement of the plate, $w(x,y)$, is expanded by the approximate natural functions of free-edge plates

$$w(x,y) = \sum_{m=1}^{M}\sum_{n=1}^{N} \zeta_{mn} f_m(x) f_n(y) \tag{11}$$

where $\zeta_{mn}$ is the complex amplitude to be determined, and $f_m(x)f_n(y)$ is the $mn$-th mode of the plate. The $f_m(x)$ and $f_n(y)$ are the natural functions of free-free beam, wherein the $f_m(x)$ is given by

$$f_m(x) = \begin{cases} 1/2 & m = 1 \\ \dfrac{1}{2}\left\{ \dfrac{\cosh(\mu_m x/a)}{\cosh\mu_m} + \dfrac{\cos(\mu_m x/a)}{\cos\mu_m} \right\} & m = 3,5,\ldots \end{cases} \tag{12}$$

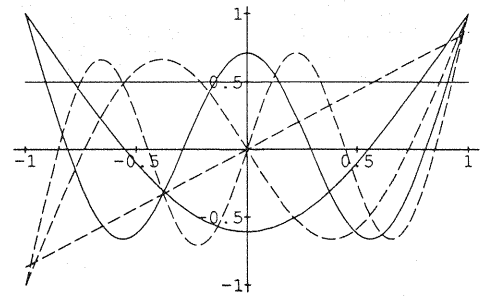


**Fig.2** Modal functions of free-free beam

$$f_m(x) = \begin{cases} \dfrac{\sqrt{3}}{2}\dfrac{x}{a} & m = 2 \\ \dfrac{1}{2}\left\{ \dfrac{\sinh(\mu_m x/a)}{\sinh\mu_m} + \dfrac{\sin(\mu_m x/a)}{\sin\mu_m} \right\} & m = 4,6,\ldots \end{cases} \tag{13}$$

where $a$ is the half length of the structure in $x$-direction, $f_m(x)$ $(m=1,2)$ are the modes corresponding to the rigid-body motions, $f_m(x)$ $(m=3,4,...)$ are the bending modal functions, and $\mu_m$ $(m=3,4,...)$ are the positive real roots of the following equations

$$\begin{cases} \tan\mu_m + \tanh\mu_m = 0 & m = 3,5,\ldots \\ \tan\mu_m - \tanh\mu_m = 0 & m = 4,6,\ldots \end{cases}. \tag{14}$$

The modal functions expressed in the equations (12) and (13) are orthogonal each other in the interval $(-a,a)$

$$\int_{-a}^{a} f_i(x) f_j(x) dx = \begin{cases} 0 & i \neq j \\ a/2 & i = j \end{cases} \tag{15}$$

The $f_n(y)$ is similarly defined as $f_m(x)$. **Fig. 2** shows some lower modes of the free-free beam, and **Fig. 3** shows some bending modes of the plate.

## 4. HYDRODYNAMIC SOLUTIONS

Under the assumption of linear wave theory, it is possible to express the complex potential, $\phi(x,y,z)$, in the form[11]

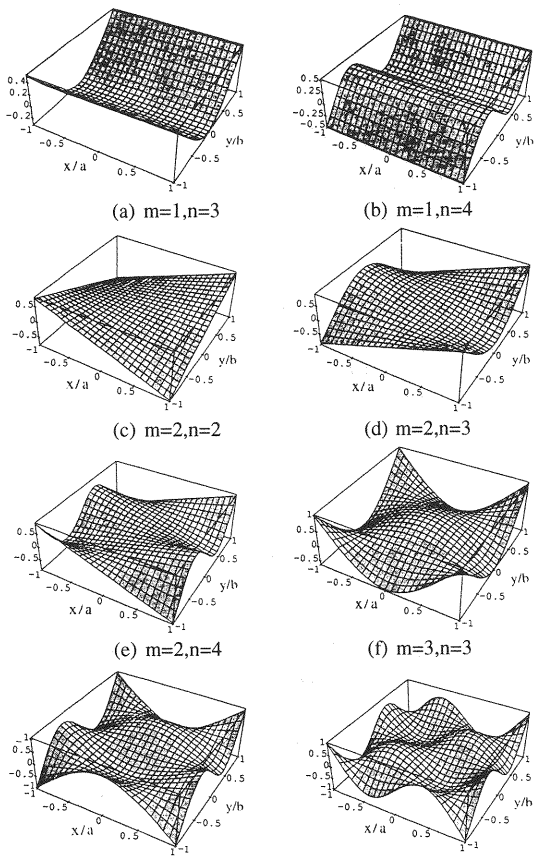


(a) m=1,n=3 (b) m=1,n=4

(c) m=2,n=2 (d) m=2,n=3

(e) m=2,n=4 (f) m=3,n=3

(g) m=3,n=5 (h) m=3,n=6

**Fig. 3** Bending modes of free-edge plate

$$\phi = \phi_D + \sum_{m=1}^{M}\sum_{n=1}^{N} \zeta_{nm}\phi_{mnR} \tag{16}$$

$$\phi_D = \phi_I + \phi_S \tag{17}$$

where $\phi_D$, $\phi_I$, $\phi_S$ and $\phi_{mnR}$ are the potentials of the diffraction wave, the incident wave, the scattering wave and the radiation wave corresponding to the unit-amplitude of *mn*-th mode, respectively.

The incident wave potential $\phi_I$ is given by

$$\phi_I = -i\frac{\xi_a g}{\sigma}\frac{\cosh\kappa(h+z)}{\cosh\kappa h}e^{i\kappa(x\cos\theta+y\sin\theta)} \tag{18}$$

where $\xi_a$ is the amplitude of incident wave, $\theta$ is the incident angle of the wave, and $\kappa$ is the wave number which follows the dispersion relation

$$\frac{\sigma^2}{g} = \kappa\tanh\kappa h. \tag{19}$$

Each of the diffraction potential $\phi_D$ and the radiation potentials $\phi_{mnR}$ must satisfy the governing equation (3), the boundary conditions (4)-(6) and the following radiation condition

$$\lim_{r\to\infty} r^{1/2}\left(\frac{\partial\phi}{\partial r} - i\kappa\phi\right) = 0 \tag{20}$$

where

$$r = \sqrt{x^2+y^2}\,. \tag{21}$$

By the expansion of Eq. (16), the boundary conditions on the wetted surface of the body can be rewritten as

$$\frac{\partial\phi_{mnR}}{\partial n} = \begin{cases} -i\sigma f_m(x)f_n(y) & \text{on } \Gamma_b \\ 0 & \text{on } \Gamma_e \end{cases} \tag{22}$$

$$\frac{\partial\phi_D}{\partial n} = 0 \quad \text{on } \Gamma \tag{23}$$

where $\Gamma=\Gamma_b+\Gamma_e$ is the total wetted surface of the plate.

According to Green's function method, the potentials, $\phi_S$ and $\phi_{mnR}$, can be expressed by the integral equation[13)]

$$2\pi\phi(\xi,\eta,\zeta) + \int_\Gamma \phi(x,y,z)\frac{\partial G}{\partial n}ds = \int_\Gamma G\frac{\partial\phi(x,y,z)}{\partial n}ds. \tag{24}$$

The function, $G(x,y,z,\xi,\eta,\zeta)$, is the Green's function given by

$$G(x,y,z;\xi,\eta,\zeta) = \frac{1}{R}+\frac{1}{R_1} + 2\int_0^\infty \frac{(\mu+\nu)e^{-\mu h}\cosh\mu(z+h)\cosh\mu(\zeta+h)J_0(\mu r)}{\mu\sinh(\mu h)-\nu\cosh(\mu h)}d\mu + i\frac{2\pi(\kappa^2-\nu^2)}{\kappa^2 h-\nu^2 h+\nu}\cosh\kappa(z+h)\cosh\kappa(\zeta+h)J_0(\kappa r) \tag{25}$$

where $J_0$ is the Bessel function of the first kind of order zero, and

$$R = \sqrt{r^2+(z-\zeta)^2} \tag{26}$$

$$R_1 = \sqrt{r^2+(2h+z+\zeta)^2} \tag{27}$$

$$\nu \equiv \frac{\sigma^2}{g} = \kappa\tanh(\kappa h). \tag{28}$$

The integral equation (24) can be solved by the boundary element method. In this paper, the constant element is employed. That is, if we divide the wetted surface of the body into a finite number of panel elements, $\Delta S_j$ ($j$=1,2,...,$N$), and let Eq.(24) is satisfied at the center of each panel element, then the integral equation can be replaced by the following linear equation sets

$$\sum_{j=1}^{N}\alpha_{ij}\phi_j=\sum_{j=1}^{N}\beta_{ij}\frac{\partial\phi_j}{\partial n}\quad i=1,2,...,N \tag{29}$$

where $\phi_j$ is the velocity potential at the center of $j$-th panel, and

$$\alpha_{ij}=2\pi\delta(i-j)+\iint_{\Delta S_j}\frac{\partial G(x_i,y_i,z_i,\xi,\eta,\zeta)}{\partial n}dS \tag{30}$$

$$\beta_{ij}=\iint_{\Delta S_j}G(x_i,y_i,z_i,\xi,\eta,\zeta)dS \tag{31}$$

$$\delta(i-j)=\begin{cases}1 & i=j\\ 0 & i\neq j\end{cases}. \tag{32}$$

If the coefficients, $\alpha_{ij}$ and $\beta_{ij}$, defined in Eqs. (30) and (31) are evaluated, it is not difficult to obtain the numerical solutions of scattering and radiation potentials by solving Eq. (29). Fortunately, Watanabe, Wu and Utsunomiya[14] have presented an effective method for calculating the integrals in Eqs. (30) and (31). Once the diffraction potential and the radiation potentials are obtained, the wave pressure can be evaluated by Eqs. (10) and (16).

## 5. SOLUTION OF MOTION

Substituting Eqs.(10), (11) and (16) into Eq. (8), the hydroelastic equation can be rewritten as

$$\sum_{m=1}^{M}\sum_{n=1}^{N}\zeta_{mn}\left[D\nabla^4\left(f_m(x)f_n(y)\right)+\left(k-\sigma^2 m\right)f_m(x)f_n(y)\right]$$
$$=i\rho\sigma\left(\phi_D+\sum_{m=1}^{M}\sum_{n=1}^{N}\zeta_{nm}\phi_{mnR}\right). \tag{33}$$

In order to obtain the unknown constant in the above equation, the Galerkin's method is applied. Multiplying the above equation by $f_l(x)f_j(y)$ and integrating over the bottom surface of the plate, we can obtain

$$\sum_{m=1}^{M}\sum_{n=1}^{N}\zeta_{mn}\left(K_{mn,lj}-i\sigma C_{mn,lj}-\sigma^2\left(M_{mn,lj}+M_{amn,lj}\right)\right)=F_{lj}$$
$$l=1,2,...,M,\ j=1,2,...,N \tag{34}$$

where

$$K_{mn,lj}=\iint_{\Gamma_b}\left[D\nabla^4\left(f_m(x)f_n(y)\right)+k\left(f_m(x)f_n(y)\right)\right]\left(f_l(x)f_j(y)\right)dxdy \tag{35}$$

$$M_{mn,lj}=\iint_{\Gamma_b}m\left(f_m(x)f_n(y)\right)\left(f_l(x)f_j(y)\right)dxdy \tag{36}$$

$$M_{amn,lj}=-\frac{\rho}{\sigma}\iint_{\Gamma_b}\mathrm{Im}(\phi_{mnR})\left(f_l(x)f_j(y)\right)dxdy \tag{37}$$

$$C_{mn,lj}=\rho\iint_{\Gamma_b}\mathrm{Re}(\phi_{mnR})\left(f_l(x)f_j(y)\right)dxdy \tag{38}$$

$$F_{lj}=i\rho\sigma\iint_{\Gamma_b}\phi_D\left(f_l(x)f_j(y)\right)dxdy. \tag{39}$$

The $K_{mn,lj}$, $M_{mn,lj}$ and $F_{lj}$ are the generalized stiffness, mass and exciting force, respectively, and $M_{amn,lj}$ and $C_{mn,lj}$ are the generalized added-mass and damping coefficient, respectively. The unknown constants, $\zeta_{mn}$, can be obtained by solving Eq. (34), and the displacement of the plate can be determined by the equation (11).

## 6. NUMERICAL EXAMPLES AND DISCUSSIONS

It is expected that the size of the numerical models should be as same as the actual structures for investigating the behaviors of the floating airports in waves. For an actual structure having several kilometers, however, large computer memories are required. Considering the capacity of the computer used herein, we consider a model which will be used for ocean test.

The model is designed by the Committee of Mega-Floating Structure of Japan. The ocean test will be performed in the Yokosuka bay where the mean water depth is 9m approximately. The structure is a box-like pontoon having a length of 300m, a width of 60m and a height of 2m. The mass of the plate per unit area is 0.5ton/m$^2$, and the stiffness of the plate is 7.5x10$^6$kNm$^2$/m. The draft of the plate is 0.5m. The plate is moored by dolphing system. In this analysis, the plate is considered to be constrained in the horizontal direction but the motions in the vertical direction are free. In order to investigate the influence of plate rigidity, the plate rigidities of 7.5x10$^5$, 7.5x10$^7$, 7.5x10$^8$, 7.5x10$^{10}$kNm$^2$/m and infinite

**Table 1** Modal amplitude of displacement of plate

| conditions | | m=1 | m=2 | m=3 | m=4 | m=5 | m=6 | m=7 | m=8 |
|---|---|---|---|---|---|---|---|---|---|
| | n=1 | 0.1035 | 0.2252 | 0.1907 | 0.3454 | 0.3659 | 0.0986 | 0.0198 | 0.0129 |
| θ=0° | n=2 | 0.0000 | 0.0000 | 0.000 | 0.0000 | 0.0000 | 0.0000 | 0.0000 | 0.0000 |
| $t$=6s | n=3 | 0.0006 | 0.0010 | 0.0012 | 0.0042 | 0.0079 | 0.0038 | 0.0030 | 0.0016 |
| $D$=7.5x10$^6$ | n=4 | 0.0000 | 0.0000 | 0.0000 | 0.0000 | 0.0000 | 0.0000 | 0.0000 | 0.0000 |
| | n=1 | 0.2739 | 0.5137 | 0.5303 | 0.7159 | 0.3099 | 0.1535 | 0.0730 | 0.0203 |
| θ=0° | n=2 | 0.0000 | 0.0000 | 0.0000 | 0.0000 | 0.0000 | 0.0000 | 0.0000 | 0.0000 |
| $t$=12s | n=3 | 0.0005 | 0.0009 | 0.0064 | 0.0080 | 0.0016 | 0.0018 | 0.0026 | 0.0021 |
| $D$=7.5x10$^6$ | n=4 | 0.0000 | 0.0000 | 0.0000 | 0.0000 | 0.0000 | 0.0000 | 0.0000 | 0.0000 |
| | n=1 | 0.4309 | 0.7756 | 0.7493 | 1.3477 | 0.6684 | 0.1597 | 0.0081 | 0.0113 |
| θ=0° | n=2 | 0.0000 | 0.0000 | 0.0000 | 0.0000 | 0.0000 | 0.0000 | 0.0000 | 0.0000 |
| $t$=18s | n=3 | 0.0006 | 0.0006 | 0.0032 | 0.0040 | 0.0019 | 0.0003 | 0.0006 | 0.0002 |
| $D$=7.5x10$^6$ | n=4 | 0.0000 | 0.0000 | 0.0000 | 0.0000 | 0.0000 | 0.0000 | 0.0000 | 0.0000 |
| | n=1 | 0.7432 | 0.5655 | 2.1470 | 1.660 | 0.4787 | 0.0284 | 0.0224 | 0.0031 |
| θ=0° | n=2 | 0.0000 | 0.0000 | 0.0000 | 0.0000 | 0.0000 | 0.0000 | 0.0000 | 0.0000 |
| $t$=24s | n=3 | 0.0001 | 0.0005 | 0.0037 | 0.0035 | 0.0022 | 0.0000 | 0.0010 | 0.0001 |
| $D$=7.5x10$^6$ | n=4 | 0.0000 | 0.0000 | 0.0000 | 0.0000 | 0.0000 | 0.0000 | 0.0000 | 0.0000 |
| | n=1 | 0.1607 | 0.1687 | 0.3695 | 0.1521 | 0.0356 | 0.0062 | 0.0038 | 0.0010 |
| θ=0° | n=2 | 0.0000 | 0.0000 | 0.0000 | 0.0000 | 0.0000 | 0.0000 | 0.0000 | 0.0000 |
| $t$=6s | n=3 | 0.0001 | 0.0001 | 0.0004 | 0.0005 | 0.0007 | 0.0002 | 0.0005 | 0.0001 |
| $D$=7.5x10$^7$ | n=4 | 0.0000 | 0.0000 | 0.0000 | 0.0000 | 0.0000 | 0.0000 | 0.0000 | 0.0000 |
| | n=1 | 0.1090 | 0.2138 | 0.0847 | 0.0089 | 0.0015 | 0.0006 | 0.0002 | 0.0001 |
| θ=0° | n=2 | 0.0000 | 0.0000 | 0.0000 | 0.0000 | 0.0000 | 0.0000 | 0.0000 | 0.0000 |
| $t$=6s | n=3 | 0.0000 | 0.0000 | 0.0000 | 0.0000 | 0.0000 | 0.0000 | 0.0000 | 0.0000 |
| $D$=7.5x10$^8$ | n=4 | 0.0000 | 0.0000 | 0.0000 | 0.0000 | 0.0000 | 0.0000 | 0.0000 | 0.0000 |
| | n=1 | 0.1239 | 0.2165 | 0.0007 | 0.0001 | 0.0000 | 0.0000 | 0.0000 | 0.0000 |
| θ=0° | n=2 | 0.0000 | 0.0000 | 0.0000 | 0.0000 | 0.0000 | 0.0000 | 0.0000 | 0.0000 |
| $t$=6s | n=3 | 0.0000 | 0.0000 | 0.0000 | 0.0000 | 0.0000 | 0.0000 | 0.0000 | 0.0000 |
| $D$=7.5x10$^{10}$ | n=4 | 0.0000 | 0.0000 | 0.0000 | 0.0000 | 0.0000 | 0.0000 | 0.0000 | 0.0000 |
| | n=1 | 0.0346 | 0.1294 | 0.0714 | 0.1580 | 0.1789 | 0.0373 | 0.0144 | 0.0044 |
| θ=45° | n=2 | 0.3243 | 0.2066 | 0.4036 | 0.0928 | 0.1884 | 0.0258 | 0.0769 | 0.0154 |
| $t$=6s | n=3 | 0.0025 | 0.0025 | 0.0055 | 0.0047 | 0.0040 | 0.0034 | 0.0030 | 0.0025 |
| $D$=7.5x10$^6$ | n=4 | 0.0005 | 0.0003 | 0.0003 | 0.0001 | 0.0004 | 0.0001 | 0.0007 | 0.0002 |
| | n=1 | 0.8542 | 0.0000 | 0.0443 | 0.0000 | 0.0745 | 0.0000 | 0.0032 | 0.0000 |
| θ=90° | n=2 | 1.8820 | 0.0000 | 0.2931 | 0.0000 | 0.1354 | 0.0000 | 0.0553 | 0.0000 |
| $t$=6s | n=3 | 0.0368 | 0.0000 | 0.0048 | 0.0000 | 0.0054 | 0.0000 | 0.0046 | 0.0000 |
| $D$=7.5x10$^6$ | n=4 | 0.0042 | 0.0000 | 0.0003 | 0.0000 | 0.0003 | 0.0000 | 0.0002 | 0.0000 |

* θ=incident angle of incoming waves, $t$=wave period, $D$=plate rigidity (kNm$^2$/m)

rigidity are also analyzed. The exciting forces due to incident and scattering waves and the vertical displacement response of the plate are investigated for incoming waves of different incident angles (θ=0°, 45° and 90°) and different periods ($t$=6sec, 12sec, 18sec and 24sec). To examine the effects of three-dimensional analysis, two-dimensional analyses based on the matched eigenfunction expansion method (MEEM)[7] are carried out and comparisons are made. In the three-dimensional analysis, the wetted surface of the plate is divided into 864 panels in which on the bottom is 720 panels and on the side is 144 panels, and 32 modes ($M$=8, $N$=4) defined in the equation (11) are used. In the two-dimensional analysis, 20 terms of eigenfunction expansion are employed and 20 modes are used.[7]

To verify the convergence of the solution, the modal amplitudes defined in the equation (11) are shown in **Table 1**. When the incident wave propagates along the positive direction of the $x$-axis (θ=0°) and the plate rigidity, $D$, is

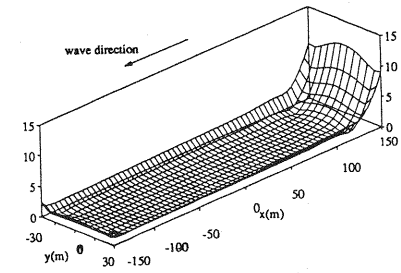


(a) θ=0°

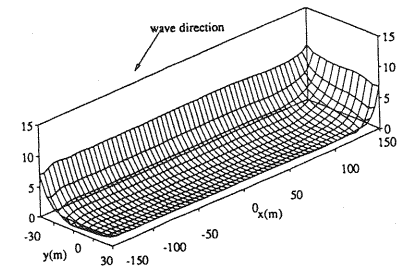


(b) θ=45°

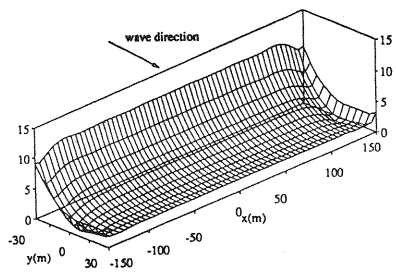


(c) θ=90°

**Fig. 4** Amplitude of diffraction wave pressure on bottom of plate (kN/m$^2$)

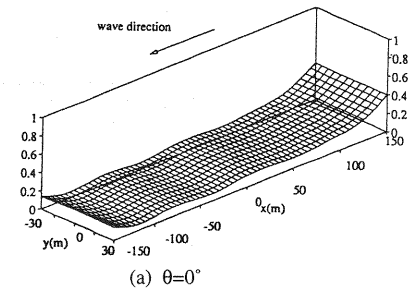


(a) θ=0°

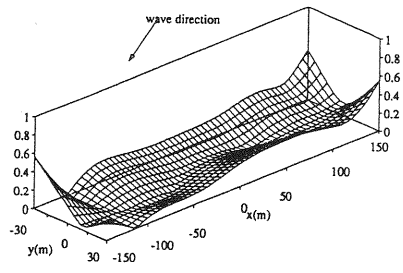


( b) θ=45°

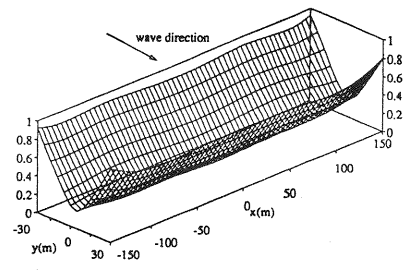


(c) θ=90°

**Fig. 5** Amplitude of displacement of plate

7.5x10$^6$kNm$^2$/m, the modal amplitudes of $m$=8 are less than 3.5%, 2.7%, 0.8% and 0.1% in comparison with the corresponding maximum values for wave period of 6sec, 12sec, 18sec and 24sec, respectively. This result indicates that the convergence becomes fast as the wave period increaese and it can be considered that the solution is converged approximately.

**Table 1** shows the influence of the plate rigidity on the convergence of the solution also. When the plate rigidity is 7.5x10$^6$, 7.5x10$^8$ and 7.5x10$^6$kNm$^2$/m, the modal amplitude of $m$=8 is less than 3.5%, 0.3% and 0.04% in comparison with the corresponding maximum values, respectively. In the case of $D$=7.5x10$^{10}$kNm$^2$/m, bending modes are approximately vanished from the motion. This indicates that the expansion of motion converges rapidly with increasing the plate rigidity.

From **Table 1**, we can also see that the modal amplitudes corresponding to diagonal bending of the plate become significant when incident angle of incoming waves is 45 degree (θ=45°) and the modal amplitudes corresponding to bending modes almost disappear when the incident waves propagate along the shorter side of the plate (θ=90°). In the case of incident waves propagating along the longer side of the plate (θ=0°), the modal amplitudes corresponding to bending modes in $y$-direction are very small.

**Table 2** Added-mass and damping coefficients due to unit heaving motion of plate

| Period (s) | Added-mass $M_a/\rho V$ | Damping $C/\rho V\sqrt{g}$ |
|---|---|---|
| 6 | 41.4 | 4.11 |
| 12 | 85.6 | 12.55 |
| 18 | 106.5 | 15.98 |
| 24 | 112.0 | 17.52 |

*$V$=water displacement

**Table 2** shows the generalized added-mass and hydrodynamic damping due to unit heaving motion. The added-masses are about 40-110 times of the physical mass of the plate, and the hydrodynamic damping is quite larger than general mechanical damping. This indicates that the plate mass and the mechanical damping appear to be relatively unimportant and have little effect on the plate response.

**Fig. 4** shows the amplitude distribution of diffraction wave pressure on the bottom of the plate. It appears that the amplitude distribution of diffraction wave pressure depends greatly on the incident angle of incoming waves and it decreases rapidly from bow to stern.

The amplitudes of displacement of the plate for unit wave amplitude are shown in **Fig. 5**. The response of the plate is sensitive to the direction of incoming waves. When $\theta$=45°, the diagonal bending of the plate becomes significant. In the case of incident waves propagating along the shorter side of the plate ($\theta$=90°), the plate moves with heave and roll approximately. When the incident waves propagate along the longer side of the plate ($\theta$=0°), the plate moves like a beam. For different wave period, the amplitudes of displacement of the plate at $y$=2.5m are shown in **Fig. 6**. The displacement increases with decreasing the wave period. **Fig. 7** shows the amplitude of displacement of the plate at $y$=2.5m for different plate rigidity. The displacement increases with decreasing the plate rigidity. In case of the plate rigidity of $D$=7.5x10$^{10}$kNm$^2$/m, the hydroelastic responses are very closed to the rigid-body responses.

In order to investigate the effect of three-dimensional and two-dimensional analysis, comparisons of the amplitude of displacement of plate between three-dimensional and two-dimensional solutions are shown in **Fig. 8**. In the case of incident wave propagating along the longer side of the plate ($\theta$=0°), the three-dimensional results are less than the two-dimensional solutions except at bow when the period of incident waves is shorter than 18sec. However, when the wave period is 24sec, in which the wave length is 223m and the structure length in the direction of wave propagation is 300m, there is a good agreement between the three-dimensional and two-dimensional solutions. The agreement can also be observed when the incident wave propagates along the shorter side of the plate for the wave period of 6sec, in which the wave length is 47m and the structure length in the direction of wave propagation is 60m. Therefore, the two-dimensional solution will have a good approximation when the incoming waves propagate along the symmetric axis of the plate and the wave length is closed to or longer than the structural length in the direction of wave propagation.

## 7. CONCLUSIONS

This paper presents the modal superposition method in the application of wave-induced response analysis of mat-like floating plates. The solution of the method consists of a solution of wave field by boundary integral equation method and an approximate Galerkin's solution of the plate. This method leads to a straightforward extension of the analysis of a rigid floating body in waves and converges rapidly.

Effects of some important parameters such as wave period, incident direction of incoming waves and plate rigidity on the response of the plate are discussed through some numerical examples. Comparisons between the two-dimensional analytical solutions and the three-dimensional solutions by the proposed method are made. Summarizing the major results, the following conclusions are obtained.

1) In the analysis of interaction between ocean waves and large floating plates, the plate mass and mechanical damping appear to be relatively less important and have little effect on the plate response than the added-mass and hydrodynamic damping.
2) The amplitude distribution of diffraction wave pressure depends greatly on the incident angle of incoming waves. The pressure due to diffraction wave decreases rapidly from bow to stern.

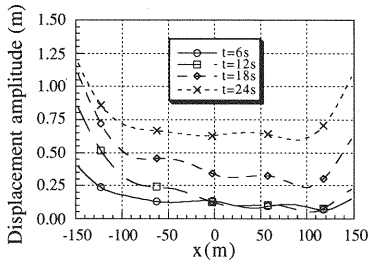


**Fig. 6** Amplitude of displacement of plate at $y$=2.5m for different wave period

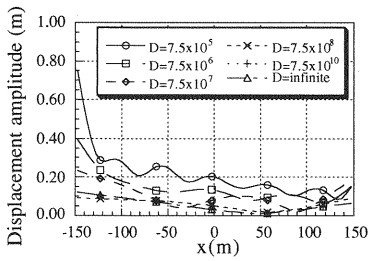


**Fig. 7** Amplitude of displacement of plate at $y$=2.5m for different plate rigidity

3) The expansion of motion converges rapidly with increasing plate rigidity. When the aspect of plate in horizontal dimension is large and incident waves propagate along the longer side of the plate, the plate moves like a beam.
4) The response of the plate is sensitive to the direction of incoming waves. At a certain range of incident angle of incoming waves, the diagonal bending of the plate becomes significant.
5) Except at the bow, the three-dimensional solutions are usually smaller than the two-dimensional solutions so that the three-dimensional analysis is expected for a short wave length. However, the two-dimensional solution will have a good approximation when the incoming waves propagate along the symmetric axis of the plate and the wave length is closed to or longer than the structural length in the direction of wave propagation.

## REFERENCES


1) Ota, H.: Offshore floating airport concept, *Proc. of 12th Ocean Engineering Symposium*, pp. 75-81, 1994 (in Japanese).
2) Wen, Y.K. and Shinozuka, M.: Analysis of floating plate under ocean waves, *Proc. of ASCE*, Vol. 98, No. WW2, pp. 177-190, 1972.


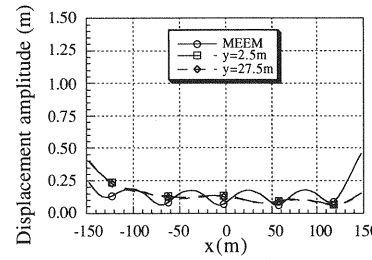


(a) θ=0, $t$=6s

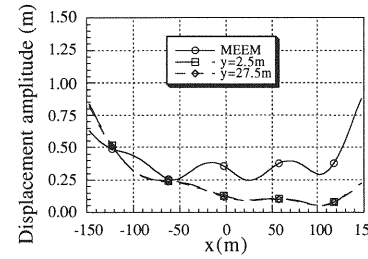


(b) θ=0°, $t$=12s

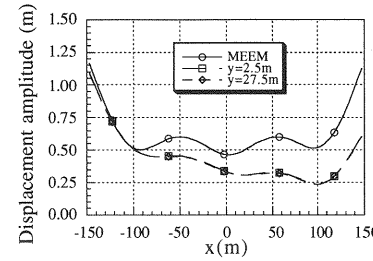


(c) θ=0°, $t$=18s

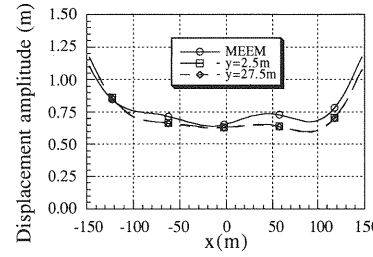


(d) θ=0°, $t$=24s

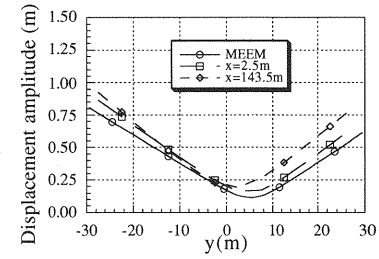


(e) θ=90°, $t$=6s

**Fig. 8** Comparison of amplitude of displacement of plate between two-dimensional and three-dimensional solutions

3) Okamoto, K., Masuda, K. and Kato, W.: Wave response analysis for huge floating structure: 1st report: dynamic interaction for fluid and elastic beam, *Proc. of Architectural of institute of Japan*, No. 314, pp. 166-175, 1982 (in Japanese).
4) Fathi, D.E.: Computation of wave induced motions on a flexible container, *Hydroelasticity in Marine Technology*, eds. Faltinsen, O. et al., Balkema, pp.301-308, 1994.
5) Utsunomiya, T., Watanabe, E., Wu, C., Hayashi, N., Nakai, K. and Sekita, K.: Wave response analysis of a flexible floating structure by BE-FE combination method, *Proc. of the Fifth International Offshore and Polar Engineering Conference*, pp.400-405, 1995.
6) Wu, C., Watanabe, E. and Utsunomiya, T.: Wave response analysis of a flexible floating structure by a simple beam model, *Proc. of Japan Society of Civil Engineers*, No.525/I33, pp. 309-317, 1995 (in Japanese).
7) Wu, C., Watanabe, E. and Utsunomiya, T.: An eigenfunction expansion matching method for analyzing wave-induced response of a large floating plate, *Applied Ocean Research*, Vol.17, pp. 310-310, 1995
8) Wen, Y.K.: Interaction of ocean waves with floating plate, *Proc. of ASCE*, Vol. 100, No. EM2, pp. 375-395, 1974.
9) Hamamoto, T., Takahashi, H. and Tanaka, Y.: An unified approach for fluid-structure interaction of flexible floating islands subjected to wind-waves and seaquakes, *J. of Structural Engineering*, No. 37B, pp. 87-99, 1991 (in Japanese).
10) Mamidipudi, P. and Webster, W.C.: The motions performance of a mat-like floating airport, *Hydroelasticity in Marine Technology*, eds. Faltinsen, O. et al., Balkema, pp. 363-375, 1994.
11) Newman, J.N.: Wave effects on deformable bodies, *Applied Ocean Research*, Vol. 16, pp.47-59, 1994.
12) Wang, S., Ertekin, R.C., Stiphou, van ATFM and Ferier, P.G.P.: Hydroelastic-response analysis of a box-like floating airport of shallow draft, *Proc. of the Fifth International Offshore and Polar Engineering Conference*, pp. 145-152, 1995.
13) Sarpkaya, M. and Isaacson, M.: *Mechanics of Wave Forces on Offshore Structures,* Van Nostrand Reinhold Company, pp. 381-466, 1981.
14) Watanabe, E., Wu, C. and Utsunomiya, T.: Wave forces on large offshore structures: an effective calculation of Green's function, *Proc. of the Fourth International Offshore and Polar Engineering Conference*, pp. 252-255, 1994.

**(Received September 18, 1995)**